Unusual magnetism of NpO_2: A study with resonant x-ray scattering

D. Mannix,* G. H. Lander, and J. Rebizant
European Commission, Joint Research Centre, Institute for Transuranium Elements, Postfach 2340, D-76125 Karlsruhe, Germany

R. Caciuffo
Istituto Nazionale per la Fisica della Materia, Dipartimento di Scienze dei Materiali della Terra, Università di Ancona, Via Brecce Bianche, I-60131 Ancona, Italy

N. Bernhoeft
Département de Recherche Fondamentale sur la Matière Condensée, Commissariat à l'Énergie Atomique-Grenoble, F-38054 Grenoble, France

E. Lidström and C. Vettier
European Synchrotron Radiation Facility, Boîte Postale 220X, F-38043 Grenoble, France
(Received 4 June 1999)

The ground state of NpO_2 has remained unresolved since the first evidence for a transition at low temperature was found in specific-heat experiments 45 years ago. Recently, muon spin relaxation measurements have shown the presence of magnetic ordering with an estimated ordered moment of $\leqslant 0.1\mu_B$/Np. Using a small (<1 mg) single crystal and photons tuned to the M_4 absorption edge of Np, we have observed the Bragg scattering from the ordered antiferromagnetic moments in NpO_2 below $T_N = 25$ K. The magnetic structure is similar to that found in UO_2, except that the moments in NpO_2 are aligned parallel to the magnetic wave vector, rather than perpendicular to it as in UO_2. No tetragonal distortion of the cubic crystal structure is found at T_N, suggesting that the magnetic structure is triple **q**. The significance for our understanding of the magnetic ground state in NpO_2 is discussed. An additional feature of these experiments, on an almost-perfect single crystal using a third-generation undulator beamline, is that we see strong effects arising from the interplay of sample absorption and the finite coherence of the incident photons that limits the full widths at half maxima of the diffraction peaks and modifies their integrated intensities. The observations are consistent with a recent theoretical treatment. [S0163-1829(99)02145-1]

I. INTRODUCTION

The actinide ion in the dioxides is known to be tetravalent (the Mössbauer isomer shift gives unambiguous evidence for this in the case of Np—see below), and, since these materials are semiconductors, it is assumed that the $5f$ states may be treated as *localized*. Using crystal-field theory the Np^{4+}:$5f^3$ configuration is expected to have two Γ_8 quartets and a Γ_6 doublet. Since it is a Kramers ion, with an odd number of $5f$ electrons, the ground state should order magnetically. Thus, it was not surprising that when the first specific-heat measurements were reported some 45 years ago[1] on NpO_2 (together with those on UO_2), the large lambdalike anomaly found at 25 K was associated with magnetic order. In 1967 susceptibility measurements showed[2] a clear maximum, again at 25 K, and a paramagnetic effective moment of $\sim 3\mu_B$/Np (as expected), so that the inferred antiferromagnetic (AF) order simply awaited a direct confirmation by Mössbauer and neutron methods. This followed rapidly for UO_2, but for NpO_2 30 years of frustration were to follow.

The corroborating experiments with the Mössbauer and neutron probes did not give the expected answers. Two independent neutron investigations[3] (on polycrystalline samples) reported no evidence for magnetic order and gave an upper limit of about $0.4\mu_B$/Np atom. The following year (1968) Mössbauer experiments[4] suggested that ordering occurred, but that the magnetic moment was only $0.01\mu_B$/Np atom; a value completely at variance with all experience at that time. A renewed attempt, using single-crystal neutron-diffraction experiments searched in vain for extra reflections involving magnetism, the last reported paper was published in 1987.[5] These experiments were difficult because the volume of the largest available single crystal of NpO_2 is about 0.6 mm^3. Further Mössbauer studies[6] concluded that the small broadening of the linewidth could be explained assuming a dynamical internal distortion of the oxygen sublattice, with no ordered moment below 25 K. However, a search for anharmonic effects in NpO_2 at low temperature by neutron diffraction[5] showed no observable deformation of either the neptunium or oxygen restoring potential at low temperature, and this excluded a dynamical distortion model.

On account of the alpha activity of transuranium elements, it is natural that much more work has been done on uranium and its compounds. UO_2 orders antiferromagnetically ($T_N = 30.8$ K) with $1.74\mu_B$/U atom,[7] and the ordering is accompanied by an *internal* distortion of the oxygen cube that surrounds the cation.[8] There is no *external* distortion from the cubic structure; i.e., the unit cell remains cubic below T_N. The magnetic structure is of type I with the magnetic wave vector $\mathbf{q} = \langle 001 \rangle$, the magnetic components are aligned perpendicular to **q**, ($\boldsymbol{\mu} \perp \mathbf{q}$). The lack of any external distortion below T_N, and any field dependence of the mag-

netic structure, suggests that UO_2 has a triple-**q** magnetic structure.[9] Inelastic neutron scattering probing the crystal-field states[10] may also be interpreted as arising from a triple-**q** configuration. A strong dynamic Jahn-Teller interaction is inferred from the neutron experiments[10] as proposed previously from an analysis of the Raman scattering by Allen[11] and the susceptibility by Sasaki and Obata.[12] There have been many ideas on why the ordered moment in NpO_2, if indeed it does exhibit long-range antiferromagnetic order, might be so small. Solt and Erdos,[13] making use of two essential elements of our understanding of UO_2, assume (a) that the crystal-field potentials are the same in UO_2 and NpO_2 apart from factors relating to the different *f*-electron count, and (b) that there is a distortion of the oxygen cage around the Np ions, which is a consequence of quadrupolar ordering [as found in UO_2 (Ref. 8)]. The first hypothesis has been substantiated by inelastic scattering experiments on NpO_2;[14] the second is not proven unambiguously, although indirect evidence for a lattice deformation is given by the observation that the ground-state quartet is split into two doublets below 25 K.[14]

One sensitive method to detect small moments is muon spin relaxation.[15] Indeed, a signal, characteristic of an antiferromagnetic state, was observed in NpO_2 below 25 K.[16] Moreover, in comparing with the signal from UO_2, the authors suggested that the AF structure of NpO_2 was like that of UO_2, type I, that the transition was second-order (as opposed to the first-order transition known to occur in UO_2), and that the ordered moment was $\sim 0.1\mu_B$/Np ion.

II. EXPERIMENTAL METHOD AND RESULTS

The experiments reported here have used resonant x-ray magnetic scattering (RXMS) to examine the antiferromagnetic structure of NpO_2. This technique exploits the large *enhancement* of the magnetically sensitive signal that occurs when the photon energy is tuned to the *M* edges in actinide materials.[17] The experiments were performed on the ID20 undulator beamline[18] of the European Synchrotron Radiation Facility (ESRF), Grenoble, France. A double crystal, Si(111), monochromator selected the appropriate x-ray energy of the Np M_4 edge of 3.845 keV. Harmonics of higher incident energy are eliminated by the use of silicon mirrors. The use of a closed-cycle refrigerator limited the base temperature to ~ 9 K. The crystal used for this work was flux grown in Karlsruhe. It is a thin (<0.25 mm) platelet of $\sim 0.7\times 0.5$ mm^2 (mass 0.73 mg) with the [001] axis perpendicular to the exposed face. Since, when working in an open laboratory such as the ESRF, the crystal must be totally encapsulated for safety reasons and normal optical methods cannot be used for alignment, orienting, and finding the crystal in the beam is nontrivial. In the special facilities in Karlsruhe the crystals are oriented and glued onto a small (2×2 mm^2) (111) Ge wafer and then sealed in a Cu capsule with a Be window. Alignment of the sample is performed as follows: we first find the (333) Bragg reflection from the Ge support wafer, and, by raster scans of the wafer across the beam (slit aperture 0.05×0.05 mm^2), determine the position of the sample as there is a strong reduction of the Bragg intensity when the photon beam is absorbed by the sample. This spatially locates the sample. Because of the strong absorption that occurs at the *M* edges all reflections must be found in Bragg geometry (i.e., scattering from the exposed face) and most of the work reported here is confined to the specular geometry involving scans around reciprocal lattice points of the type $(00L)$, but some off-specular positions were also examined. The incident aperture for most of the experiments was 0.2×0.2 mm^2, close to the focal spot size of ID20, making full use of the high brilliance of the undulator source. The beam flux at 3.845 keV is estimated as 5×10^{11} photons/sec. The crystal was of excellent quality with a mosaic of 0.01°.

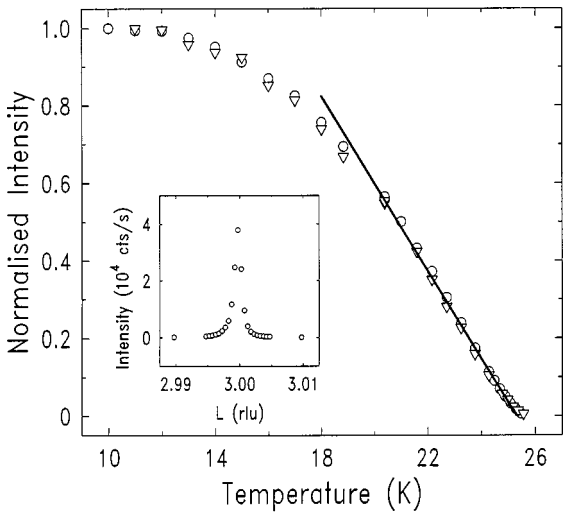

FIG. 1. Normalized temperature dependence of the (001) (open triangles) and (003) (open circles) *magnetic* Bragg intensities. The straight line corresponds to the exponent $\beta=0.5$, which is the molecular-field value, with $T_N=25.3(1)$ K. The inset shows data for the specular (003) reflection at 10 K as a function of the momentum-transfer component *L*.

In the antiferromagnetic phase at $T=10$ K a strong resonant peak ($\sim 38\,000$ counts/sec) corresponding to the (003) reflection was found; the intensity of this peak as a function of the scattered wave vector along the specular rod (i.e., a longitudinal or θ–2θ scan) and its temperature dependence are shown in Fig. 1. The peak may be identified as arising from a long-range AF structure of the Np magnetic moments both by its temperature and energy dependence (not shown). In comparison with UO_2, in which the transition is strongly first order, the transition in NpO_2 appears continuous, the ordering wave vector being the same in both cases, viz., $\mathbf{q}=\langle 001\rangle$.

Using the RXMS technique one is unable to determine the *magnitude* of the magnetic moments.[19] However, the moment directions can be determined.[20] Representing the scattering of the beam (incident wave vector $\mathbf{k}_i$, final wave vector $\mathbf{k}_f$) in matrix form so that

$$\text{amplitude } \alpha\begin{pmatrix} \sigma\rightarrow\sigma & \pi\rightarrow\sigma \\ \sigma\rightarrow\pi & \pi\rightarrow\pi \end{pmatrix}, \tag{1}$$

where σ and π represent the polarization of the photon beam in standard notation, Hill and McMorrow[20] give expressions for the different possible scattering processes. Limiting our discussion to the dipole terms, which are known to dominate

the scattering at actinide M edges,[17] the term appearing at the magnetic wave vector $\pm\mathbf{q}$ is given by

$$f^{X\ RES}_{n=1.E1} = iF^{(1)}\begin{pmatrix} 0 & z_1\cos\theta + z_3\sin\theta \\ z_3\sin\theta - z_1\cos\theta & -z_2\sin 2\theta \end{pmatrix}, \tag{2}$$

where $F^{(1)}$ gives the strength of the scattering and depends on overlap integrals between core and intermediate states.[19] The thermal evolution of the signal may be associated with the temperature dependence of the ordered moment.[21] The terms z_1, z_2, and z_3 are components of a unit vector along the direction of the magnetic moment, such that z_3 is the component along the scattering vector $\mathbf{Q}$ (defined by $\mathbf{k}_i - \mathbf{k}_f$), z_1 is the component in the scattering plane perpendicular to $\mathbf{Q}$ (defined by $\mathbf{k}_i + \mathbf{k}_f$), and z_2 is the component perpendicular to the scattering plane (defined by $-\mathbf{k}_i \times \mathbf{k}_f$). In the experiment the scattering plane is $[100]\times[001]$ and $\mathbf{Q}\|[001]$ for specular reflections. The incident polarization is σ, so that the only term expected in the cross section is that in $\sigma \rightarrow \pi$ and has an amplitude proportional to $z_1\cos\theta + z_3\sin\theta$.

At these incident photon wavelengths ($\lambda = 3.22$ Å) the amount of reciprocal space accessible is limited, but a comparison of the (001) and (003) reflections is sufficient to tell whether the projected components of the magnetic moment are parallel to $\mathbf{q}$ or lie in the scattering plane perpendicular to $\mathbf{q}$. These are the only two possibilities allowed on symmetry arguments as the symmetry of the magnetic cell must be tetragonal (or lower). With $\boldsymbol{\mu}\|\mathbf{q}$ the expected scattering amplitude should change as $(z_3\sin\theta)$, whereas with $\boldsymbol{\mu}\perp\mathbf{q}$ the amplitude should change as $(z_1\cos\theta)$. Since the (003) intensity is observed to be greater than that at the (001) position our initial estimate is that the configuration is $\boldsymbol{\mu}\|\mathbf{q}$. However, after standard corrections for the Lorentz factor, beam footprint, and absorption, the integrated intensities deviated strongly from the expected $(\cos\theta)^2$ dependence predicted above. Furthermore, the *width* [hereafter used to mean full width at half maximum (FWHM)] of the (001), (002), and (003) reflections were all markedly different even though over this region of Q space the instrumental resolution is essentially constant.

III. PROBE COHERENCE EFFECTS ON THE MEASUREMENTS

When the beam coherence of the incident radiation approaches the length scale of the sample correlation length and/or the absorption length a more careful interpretation of the data is required.[22] In particular, at the actinide M edges the role of absorption is crucial as has been verified by performing scans as a function of the incident photon energy, which changes the absorption length in a systematic way.[23] Here we are not concerned with energy space, but, as a consequence of having a crystal of high perfection, must examine more carefully the effects in diffraction space when performing q scans away from the Bragg peak. For the sake of simplicity we shall confine our discussions to longitudinal scans, i.e., parallel to the momentum transfer $\mathbf{Q}$. To avoid the problems of absorption, we have used 8-keV photons to measure the width of the Bragg charge reflections from the crystal and find for the specular (006) a value of 6×10^{-4} reciprocal lattice units (rlu). Neglecting resolution effects this shows that the longitudinal coherence length of the beam and/or the spatial correlation length of the atomic order in the crystal is at least $\zeta \sim 0.3$ μm, and may be longer.

The estimated incident beam longitudinal coherence length parallel to $\mathbf{k}_i$ is given by $\xi = \lambda/(\Delta\lambda/\lambda) \sim 3\mu$m at the resonant energies of these experiments, and about half this value at 8 keV. Since the spatial perfection of the crystal is of the same order of magnitude, removing the resolution function of the instrument is not straightforward and account must be taken of the beam coherence. In principle, we cannot measure a correlation length greater than the beam coherence. The last length scale of importance is that given by the absorption, and is defined by $1/\mu$ as the distance through which the beam intensity suffers a $1/e$ attenuation on passing through the sample. With a photon energy of 8 keV $\mu \sim 4000$ cm^{-1} for uranium with a density of 19 g/cm^3; UO_2 and NpO_2 have actinide densities of ~ 10 g/cm^3 so that for these materials $1/\mu \sim 5$ μm. At 8 keV the absorption length is sufficiently long that it does not significantly reduce the beam intensity within a single coherence volume. However, as the resonant energy is approached, the absorption greatly increases. At the M absorption edges in UO_2 the values of μ approach 5×10^4 cm^{-1} and 9×10^4 cm^{-1} at the M_4 and M_5 edges, respectively.[24] These high values translate into $1/\mu$ values of 0.20 μm and 0.11 μm, respectively. The absorption lengths then become the *shortest* length scale in the problem, and it is the shortest length scale that determines the shape and form of the peaks in both energy and q space.

As shown in Ref. 22, when the absorption on the length of one atomic spacing, i.e., μa, where a is the plane spacing, is small, but the total absorption within the diffracting volume of the crystal is large, which is the case here, then the intensity as a function of $\mathbf{q}$ and energy E is given by

$$I(q,E)\alpha\left[\frac{\Gamma^2}{\Gamma^2+(\Delta E-E)^2}\right] \times\left[\frac{1+e^{-2\mu^* Na}-e^{-\mu^* Na}\{2\cos(qNa)\}}{\mu^{*2}+q^2}\right], \tag{3}$$

where Γ is the effective inverse lifetime of the scattering process, ΔE the energy step between the initial and intermediate state of the resonant process, E the incident photon energy, q is the wave-vector offset from the Bragg condition, and

$$\mu^* = \frac{\mu}{2}\left(\frac{1}{\sin\alpha}+\frac{1}{\sin\beta}\right). \tag{4}$$

Here α and β are the incident angle and exit angle from the face of the crystal in which the planes of d space a are arranged perpendicular to the surface normal. For specular reflections, in which $\alpha = \beta$, this simplifies to $\mu^* = \mu/\sin\alpha$. As q is small, we will assume that $\cos(qa)$ is close to one.

At the resonant energy the first factor of Eq. (3) is constant, and we focus on the specular wave-vector profile of the diffraction peaks [i.e., $I(q, E = E_{res})$ in Eq. (3)]. Considering the incident *beam* as a sum of *rays*, where, with each ray there is associated a coherent diffraction volume,[22] one sees

TABLE I. Calculated intensities as a function of the two possible moment directions for the two specular reflections as measured at the M_4 resonant energy in NpO_2. Case *A* corresponds to the standard relationship, whereas case *B* corresponds to that developed above and expressed in Eq. (6). The intensities have been normalized to that of the strongest reflection in each case. The observed ratio $I(001)/I(003)=0.04(1)$.

	$\boldsymbol{\mu}\parallel\mathbf{q}$		$\boldsymbol{\mu}\perp\mathbf{q}$	
hkl	*A*	*B*	*A*	*B*
(001)	16	5	100	100
(003)	100	100	16	49

that for a given reflection, magnetic or charge, the measured intensity profile may be considered to arise from two distinct contributions. First, there is the (coherent) diffraction process of a given ray, second there is the incoherent summation over the individual diffracted rays collected in the detector at a given setting of the spectrometer. The conventional analysis,[25] for monochromatic sources and monocrystalline samples, assumes that the ray coherence volume is sufficiently large that it may be removed from consideration and that the scattering is dominated by finite-size effects of the sample (e.g., mosaic block dimension) and the instrumental resolution function (i.e., the angular distribution of the rays within the beam). The measured profile is then represented by a convolution, at the level of intensities, of sample response function and spectrometer resolution function. Absorption is likewise treated at the level of intensities. This gives a correction *linear* in the optical path traversed by the beam. In Bragg reflection geometry, from a semi-infinite sample, the absorption correction may then be represented by the response of a nonabsorbing sample of thickness given by the characteristic absorption length.

In the case of strong absorption, when $1/\mu$ is the shortest length scale in the problem, this approach fails. It fails to give account of the diffraction profile at a given Bragg point, it fails to account for the relative intensities between Bragg points, and it fails to describe the absorption process correctly. In this limit the observed intensity may no longer be represented by the convolution of sample and spectrometer response functions and the width of the diffraction peaks in wave-vector space becomes a measure of the characteristic absorption length. This is apparent from Eq. (3) since, in the extreme limit $\mu^* Na \to \infty$ when the exponential terms in the numerator are negligible, one has

$$I_{res}(q)\alpha\left[\frac{1}{\mu^{*^2}+q^2}\right]. \tag{5}$$

In this limit the width gives *no* information on the spatial correlations in the material since these are tied to *N* in the numerator. Further, since μ^* depends on the scattering angle, see Eq. (2), the widths of the diffraction profiles acquire an angular dependence over and above that given by the standard footprint [proportional to $1/\sin(\alpha)$] and Lorentz $[1/\sin(\theta)]$ corrections for specular scans in the Bragg geometry. Thus, finally we may write

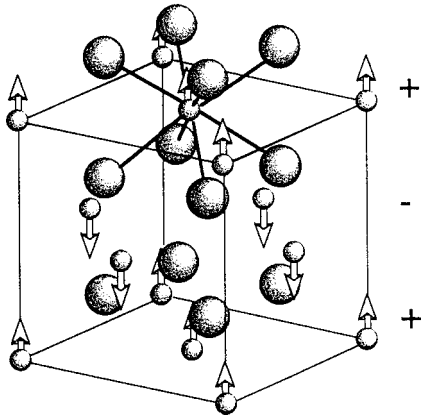

FIG. 2. The fluorite crystal structure of NpO_2 is shown. The larger circles represent oxygen, and the 8 oxygen atoms surrounding the Np atom on the top face are shown. The arrows indicate the components of the magnetic structure propagating along the [001] axis. This is a simple $+-+-$ (type-I) alternating sequence of ferromagnetic planes. The real magnetic structure is triple-**q**, i.e., all three equivalent $\langle 001\rangle$ components exist simultaneously.

$$I_{res}(q)\alpha\left(\frac{1}{\sin\alpha\,\sin\theta}\right)\left[\frac{1}{\mu^{*^2}+q^2}\right]. \tag{6}$$

(Recall that the scans here are longitudinal in reciprocal lattice units—the term $\sin\theta$ then replaces the more standard $\sin 2\theta$ in the Lorentz factor.) We may now calculate the intensity ratios of the (001) and (003) magnetic Bragg reflections for the different moment directions, and these values, both for the standard relationship and that based on Eq. (6) are given in Table I.

From this table and the observed ratio we conclude that $\boldsymbol{\mu}\parallel\mathbf{q}$. Moreover, the intensities fit *only* with the formulas (case *B*) taking into account the coherence of the beam and the large absorption, as discussed above. We have also examined the (102) off-specular reflection. Its intensity is some 50% of the (003). This is more complex to calculate within the probe coherence model. The intensity is compatible with the $\boldsymbol{\mu}\parallel\mathbf{q}$ configuration, but not with $\boldsymbol{\mu}\perp\mathbf{q}$, since in this latter case the (102) reflection would have an intensity of less than

TABLE II. Parameters deduced by fitting Eq. (3) to the line shapes of both charge (002) and magnetic (001) and (003) Bragg reflections (as shown in Fig. 3). Δ_{obs} is the observed FWHM, which is independent of temperature. *N* is the total number of atomic planes and *L* is the deduced correlation length. The errors on the deduced quantities in the table are between 5% and 10%, except where marked as referring to the least significant digit.

	$(hk\ell)$	$\sin\theta$	Δ_{obs} (10^3 rlu)	$10^4\,\mu$ (Å^{-1})	*N*	*L* (Å)
M_4 edge	(001)	0.297	3.1(2)	4.0	335	6200
	(002)	0.593	1.35(10)	3.9	990	9100
	(003)	0.890	0.96(5)	4.8	1100	6700
M_5 edge	(002)	0.623	1.73(8)	6.4	940	8200
	(003)	0.934	1.58(8)	8.0	1100	6400

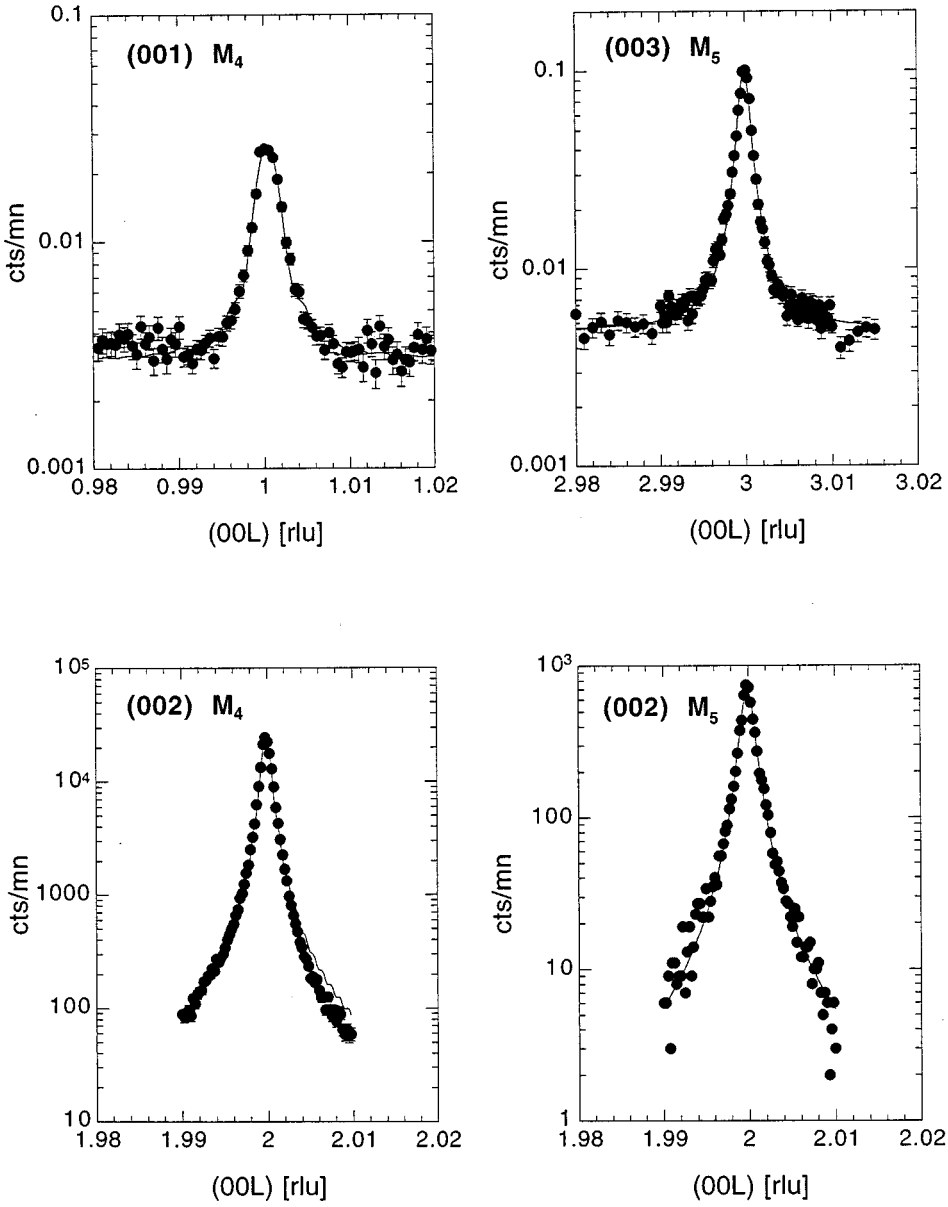

FIG. 3. Intensity at the Np M resonances for two charge and two magnetic reflections as a function of the wave-vector offset from the Bragg position. The solid lines are the result of taking into account the interplay between sample absorption and the finite coherence of the incident photons, as described in the text, and in Eq. (3). The parameters from the fits are given in Table II.

5% of the (003) for both the standard and coherence models. Note that the wave vector $\mathbf{q}=[100]$ at the (102) reflection.

The magnetic structure, as deduced so far in our experiments, of NpO_2 is shown in Fig. 2. It is very similar to that in UO_2, except that the moment directions are along the propagation vector in NpO_2 and perpendicular to it in UO_2. We shall show later that the correct magnetic structure of NpO_2 is almost certainly triple **q**, so that the illustration in Fig. 2 is of one component of this structure.

We now return to a detailed consideration of the line shapes at the M_4 and M_5 edges. Assuming the spectra to be dominated by the absorption effect, the measured line shapes at the M_4 and M_5 edges have been fitted with the full formula Eq. (3) to extract values of μ and N. The values are given in Table II and representative peaks at both the M_4 and M_5 edges are shown in Fig. 3. The role of the spectrometer resolution (at the level of intensities) has been estimated following Appendix C of Ref. 22 and found negligible.

From Table II one deduces a value of $\mu=(4.2\pm0.4)\times10^{-4}$ Å^{-1} at the M_4 edge and $\mu=(7.2\pm0.8)\times10^{-4}$ Å^{-1} at the M_5 edge. The magnetic correlation range is deduced to be slightly smaller than the value for the charge peaks; 6400 Å in comparison with 8700 Å. This reduced magnetic correlation length is most likely related to an average domain dimension perpendicular to the sample surface. The correlation length of the charge peaks may be limited by the mosaic block dimension or the probe coherence length; it is not possible to distinguish the two effects at this level. We find no temperature dependence to the widths.

IV. STRUCTURAL BEHAVIOR

A major question in NpO_2 is whether there is a structural distortion at T_N. Inelastic neutron scattering[14] showed a splitting of the ground state Γ_8 quartet below T_N that was attributed to a structural distortion, either external (i.e., a reduction in the total symmetry; for example, from cubic to tetragonal) or internal [as found in UO_2 (Ref. 8)]. Using 8-keV photons together with a Ge analyzer we have monitored the position and width of the (006) charge reflection as

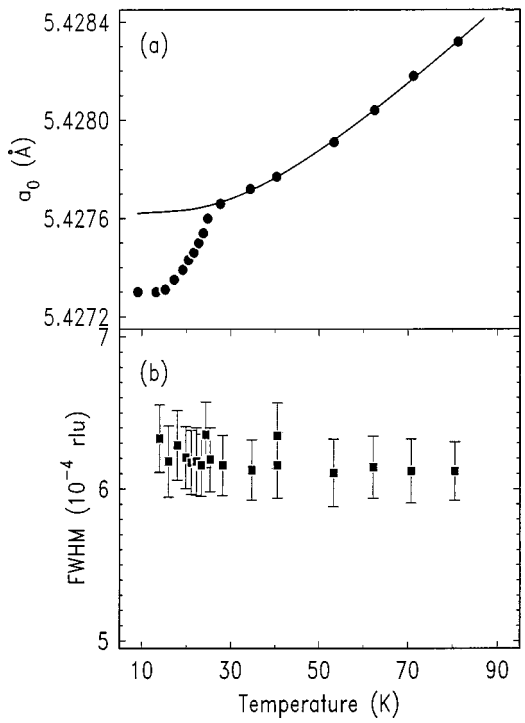

FIG. 4. (a) The variation with temperature of the lattice parameter, measured at the charge (006) reflection with 8-keV photons and a Ge analyzer. The solid line is the fit to Eq. (7) as described in the text. (b) Width of the (006) reflection as a function of temperature.

a function of temperature. The position of this reflection gives the lattice parameter as shown in Fig. 4(a). The width is shown in Fig. 4(b) and does not change on passing through T_N. Our conclusion is that any *external* distortion is $|(a-c)/a|<10^{-4}$. In particular, with the magnetic symmetry (see Fig. 2) we would anticipate a tetragonal distortion. This would result in a splitting (or at least a broadening of the FWHM) of the charge (006) reflection. It is this absence of any change in the FWHM on passing through T_N that suggests there is no tetragonal distortion and hence a triple-**q** magnetic structure in NpO_2. The triple-**q** configuration has cubic symmetry.[9] These measurements have been made with 8-keV photons that have a penetration sufficiently great to probe more than one possible magnetic domain.

Internal distortions may be either homogeneous or inhomogeneous. The former correspond to the normal modes of the oxygen cube and, if present, give rise to *changes* in the intensities of the fluorite-structure peaks. No new reflections will appear. In our x-ray experiment it is difficult to measure any such changes, and we rely on the neutron examination[5] that gave an upper value of ~ 0.008 Å for any such deformation. On the other hand, inhomogeneous deformations, such as observed in UO_2, result from combinations of normal modes and give rise to superstructure reflections. We have examined a number of positions in reciprocal space, (005), (105), (205), (104), and (114), at which internal distortions of the oxygen tetrahedra might give rise to superstructure peaks below T_N. Any ''extra'' intensity was estimated at $\leqslant 10^{-8}$ of the charge intensities. Based on the magnitude of the internal distortion in UO_2 we would expect ''extra'' intensity at the level of $\sim 10^{-5}$ of the charge peaks, so our sensitivity is some three orders of magnitude lower, translating into an amplitude of ~ 0.03 times less than the oxygen shift in UO_2, which gives an upper limit of 4×10^{-4} Å. This is 100 times smaller than the zero-point motion. Of course, in setting these limits one should be aware that the searches can never be made exhaustively over the whole Brillouin zone, and in this case were constrained to positions corresponding to $|\mathbf{q}|=1$, corresponding to the magnitude of the magnetic wave vector.

The lattice thermal expansion above T_N is typical for a solid and can be modeled by the relationship

$$a(T)=a_0\left\{1+\frac{\alpha T_E}{2}\left[\coth\left(\frac{T_E}{2T}\right)-1\right]\right\}, \tag{7}$$

which is obtained from the Grüneisen approximation for the anharmonic effects, and the Einstein model for the constant-volume specific heat; a_0 is the lattice parameter at $T=0$, T_E is the Einstein temperature, and α is the linear thermal expansion coefficient for $T\gg T_E$. These parameters should only be considered as qualitative; the range of investigated temperature being too small to allow a quantitative analysis. A disagreement with data taken at much higher temperature[26] is not significant. The solid line in Fig. 4(a) shows the values obtained from Eq. (7) for $T_E=106$ K and $\alpha=3\times 10^{-6}$ K^{-1}. It is evident that an anomalous contraction of the unit cell occurs on cooling below T_N, corresponding to a relative volume variation $\Delta V/V=1.8(2)\times 10^{-4}$.

A similar, but smaller, volume contraction has been observed in UO_2, where a discontinuity $\Delta V/V$ of about 7×10^{-5} has been measured at T_N using strain-gauge techniques.[27] This effect has been attributed to magnetoelastic interactions and is predicted to be proportional to the expectation value of the T_{xy} quadrupolar operator.[11] The results shown in Fig. 4(a) can therefore be taken as evidence that quadrupolar ordering accompanies the establishment of AF order in NpO_2.

V. CONCLUSIONS

Our experiments have made a major step forward in understanding the antiferromagnetism of NpO_2. Although the RXMS technique cannot give the ordered moment, the value seems reasonably well established between 0.01 and $0.10\mu_B$ from ^{237}Np Mössbauer spectroscopy and muon experiments. Furthermore, it appears *long range* in extent (in fact our lower limit is ~ 6000 Å for the spatial magnetic correlations, and they may be longer), so different to that found, and also involving a small moment, in URu_2Si_2,[28] where the magnetic correlation length extends only ~ 400 Å.

Our findings are in good agreement with those reported by muons.[16] The AF structure has the same wave vector and is of the triple-**q** type as found in UO_2, but the moment direction is different. The transition at T_N is continuous in NpO_2 whereas discontinuous in UO_2. To obtain an almost zero moment in the framework of the Solt and Erdös model,[13] the magnetic moment must lie parallel to **q**, as we have found. However, the calculations in Ref. 13 were performed assuming a single-**q** model for the magnetic structure and a monoclinic distortion of the oxygen cage. If the magnetic structure is triple-**q**, as we suggest, then the arguments

leading to a small moment may not necessarily apply. Moreover, there is no measurable monoclinic distortion. Thus, even though we now know that AF order exists, in our view the explanation of the small ordered moment remains unanswered.

In these experiments, using an undulator beam from a third-generation synchrotron source and an extremely good crystal, we have encountered an interesting situation in that the probe coherence length of the photon beam is *greater* than the absorption length of the photon at the resonant energies. This leads to some unusual effects; notably that one cannot perform a convolution of the sample and probe response functions to obtain the measured response. The FWHM's of the diffraction peaks vary as a function of Bragg angle in a way incompatible with the instrumental resolution, and the intensities calculated using standard formulas do not agree with our expectations. These inconsistencies are resolved by using formulas recently developed in Ref. 22 in which the probe coherence of the photon beam is included explicitly. The fits to the line shapes, as shown in Fig. 3, are excellent over more than two decades in intensity.

Historically, NpO_2 was the first of the so-called ''small $5f$ moment systems'' to be discovered. Recently, this phenomenon has arisen again in *metallic* heavy-fermion systems, such as UPt_3, URu_2Si_2.[15,29] In these cases magnetic moments may be imagined to be quenched by the Kondo interaction, i.e., via an interaction between the pseudolocalized f electrons and the conduction-electron states. Such an interaction is unlikely in semiconducting NpO_2, so that the answer must lie elsewhere. To our knowledge the only other similar system (in the sense that crystal-field effects are more important than Kondo interactions) with small magnetic moments is UPd_3.[30] In this material there is a small ordered moment and complicated quadrupolar ordering. Hopefully our experiments, and those using muons, on NpO_2 will stimulate new thoughts on an old problem.

ACKNOWLEDGMENTS

We thank Giuseppe Amoretti and Paolo Santini for discussions and we acknowledge the help and cooperation of the Radioprotection staff at the European Synchrotron Radiation Facility during the course of these experiments.

*Also at European Synchrotron Radiation Facility, B.P. 220X, F-38043 Grenoble, France.

[1] E. F. Westrum, J. B. Hatcher, and D. W. Osborne, J. Chem. Phys. **21**, 419 (1953); D. W. Osborne and E. F. Westrum, *ibid.* **21**, 1884 (1953).

[2] J. W. Ross and D. J. Lam, J. Appl. Phys. **38**, 1451 (1967).

[3] D. E. Cox and B. C. Frazer, J. Phys. Chem. Solids **28**, 1649 (1967); L. Heaton, M. H. Mueller, and J. M. Williams, *ibid.* **28**, 1651 (1967).

[4] B. D. Dunlap, G. M. Kalvius, D. J. Lam, and M. B. Brodsky, J. Phys. Chem. Solids **29**, 1365 (1968).

[5] R. Caciuffo, G. H. Lander, J. C. Spirlet, J. M. Fournier, and W. F. Kuhs, Solid State Commun. **64**, 149 (1987).

[6] J. M. Friedt, F. J. Litterst, and J. Rebizant, Phys. Rev. B **32**, 257 (1985).

[7] B. C. Frazer, G. Shirane, D. E. Cox, and C. E. Olsen, Phys. Rev. **140**, A1448 (1965); B. T. M. Willis and R. I. Taylor, Phys. Lett. **17**, 188 (1965).

[8] J. Faber and G. H. Lander, Phys. Rev. B **14**, 1151 (1976).

[9] P. Burlet, J. Rossat-Mignod, S. Quezel, O. Vogt, J. C. Spirlet, and J. Rebizant, J. Less-Common Met. **121**, 121 (1986).

[10] G. Amoretti, A. Blaise, R. Caciuffo, J. M. Fournier, M. T. Hutchings, R. Osborn, and A. D. Taylor, Phys. Rev. B **40**, 1856 (1989).

[11] S. J. Allen, Phys. Rev. **166**, 530 (1968); **167**, 492 (1968).

[12] K. Sasaki and Y. Obata, J. Phys. Soc. Jpn. **28**, 1157 (1970).

[13] G. Solt and P. Erdös, J. Magn. Magn. Mater. **15-18**, 57 (1980).

[14] G. Amoretti, A. Blaise, R. Caciuffo, D. Di Cola, J. M. Fournier, M. T. Hutchings, G. H. Lander, R. Osborn, A. Severing, and A. D. Taylor, J. Phys.: Condens. Matter **4**, 3459 (1992).

[15] See, for example, R. H. Heffner, J. Alloys Compd. **213-214**, 232 (1994).

[16] W. Kopmann, F. J. Litterst, H.-H. Klauss, M. Hillberg, W. Wagener, G. M. Kalvius, E. Schreier, F. J. Burghart, J. Rebizant, and G. H. Lander, J. Alloys Compd. **271-273**, 463 (1998).

[17] E. D. Isaacs, D. B. McWhan, C. Peters, G. E. Ice, D. P. Siddons, J. B. Hastings, C. Vettier, and O. Vogt, Phys. Rev. Lett. **62**, 1671 (1989); D. B. McWhan, C. Vettier, E. D. Isaacs, G. E. Ice, D. P. Siddons, J. B. Hastings, C. Peters, and O. Vogt, Phys. Rev. B **42**, 6007 (1990); C. Vettier, J. Magn. Magn. Mater. **129**, 59 (1994); G. H. Lander, J. Alloys Compd. **250**, 544 (1997).

[18] A. Stunault, C. Vettier, F. de Bergevin, N. Bernhoeft, V. Fernandez, S. Langridge, E. Lidström, J. E. Lorenzo-Diaz, D. Wermeille, L. Chabert, and R. Chagnon, J. Synchrotron Radiat. **5**, 1010 (1998).

[19] J. P. Hannon, G. T. Trammell, M. Blume, and D. Gibbs, Phys. Rev. Lett. **61**, 1245 (1988).

[20] J. P. Hill and D. F. McMorrow, Acta Crystallogr., Sect. A: Found. Crystallogr. **52**, 236 (1996).

[21] J. Luo, G. T. Trammell, and J. P. Hannon, Phys. Rev. Lett. **71**, 287 (1993).

[22] N. Bernhoeft, Acta Crystallogr., Sect. A: Found. Crystallogr. **55**, 274 (1999).

[23] N. Bernhoeft, A. Hiess, S. Langridge, A. Stunault, D. Wermeille, C. Vettier, G. H. Lander, M. Huth, M. Jourdan, and H. Adrian, Phys. Rev. Lett. **81**, 3419 (1998).

[24] J. O. Cross, M. Newville, J. J. Rehr, L. B. Sorensen, C. E. Bouldin, G. Watson, T. Gouder, G. H. Lander, and M. I. Bell, Phys. Rev. B **58**, 11 215 (1998).

[25] B. E. Warren, *X-ray Diffraction* (Addison-Wesley, Reading, MA, 1969).

[26] H. Serizawa, Y. Arai, M. Takano, and Y. Suzuki, J. Alloys Compd. **282**, 17 (1999).

[27] O. G. Brandt and C. T. Walker, Phys. Rev. Lett. **18**, 11 (1967).

[28] E. D. Isaacs, D. B. McWhan, R. N. Kleiman, D. J. Bishop, G. E. Ice, P. Zschack, B. D. Gaulin, T. E. Mason, J. D. Garrett, and W. J. L. Buyers, Phys. Rev. Lett. **65**, 3185 (1990).

[29] G. Aeppli and C. Broholm, in *Handbook on the Physics of Rare Earths*, edited by K. A. Gschneidner, L. Eyring, G. H. Lander, and G. Choppin (Elsevier, Amsterdam, 1994), Vol. 19, p. 123.

[30] K. A. McEwen, U. Steigenberger, K. N. Clausen, J. Kulda, J-G. Park, and M. B. Walker, J. Magn. Magn. Mater. **177-181**, 37 (1998).